

*Regular Article***A Design of Similar High-gain and Dual-band Frequency/Polarization Reconfigurable Antenna for ISM Band Applications**Cong Danh Bui¹, Minh Thuan Doan², Thi Thanh Kieu Nguyen³, Truong Khang Nguyen^{1,4}¹ Faculty of Electrical and Electronics Engineering, Ton Duc Thang University, Ho Chi Minh City, Vietnam² Faculty of Electrical and Electronics Engineering, Bach Khoa University, Ho Chi Minh City, Vietnam³ Faculty of Engineering, Binh Thuan College, Binh Thuan, Vietnam⁴ Division of Computational Physics, Institute for Computational Science, Ton Duc Thang University, Ho Chi Minh City, Vietnam

Correspondence: Truong Khang Nguyen, nguyentruongkhang@tdtu.edu.vn

Communication: received 21 June 2021, revised 13 August 2021, accepted 10 May 2022

Online publication: 12 May 2022, Digital Object Identifier: 10.21553/rev-jec.274

The associate editor coordinating the review of this article and recommending it for publication was Prof. Vo Nguyen Quoc Bao.

Abstract– This paper proposes a frequency/polarization reconfigurable antenna (RA) incorporating Frequency Selective Surface (FSS) to achieve dual-band and similar high-gain characteristics. The proposed RA-FSS design using 4 PIN Diodes can produce reconfigurability between circular polarization (CP) at 1.8 GHz and linear polarization (LP) at 2.45 GHz. The fabricated prototype shows good CP performance at 1.8 GHz while the measured peak broadside gains are about 7.2 dBi at 1.8 GHz and 8.5 dBi at 2.45 GHz when PIN diode ON and OFF, respectively.

Keywords– Reconfigurable antenna, Frequency Selective Surface, Microstrip antenna, PIN Diode.

1 INTRODUCTION

Reconfigurable antenna (RA) has attracted a lot of research attention nowadays [1, 2]. By using active components such as PIN Diode, Varactor Diode, RF-MEMS, etc., the antenna can adjust its characteristics namely operating frequency [3], polarization [4], radiation pattern [5], etc. Two operating modes, ON and OFF, of PIN Diode, can be changed alternatively with fast speed and create a wide range of modifications for frequency and polarization reconfigurable antenna, which are their well-known advantages. Frequency RA can significantly reduce the number of antennas in a system that supports multiple protocols such as GSM, GPS, WiFi, etc. by easily switching between operating frequencies. In addition, polarization RA, especially when alternates linear and circular polarization, can improve signal quality in a non-ideal environment and system capacity. One disadvantage of RA is the DC bias line, which is used to control active components. The resistors required for bias circuits and internal ones existing in active components create power loss in the antenna and thus, reduce the radiation efficiency in RA compared to conventional ones. Therefore, we introduce a frequency selective surface (FSS) as a solution for radiation efficiency improvement.

Since first introduced in 1956 by G. V. Trentini [6], FSS has been studied extensively over the years [7–9]. One of the most interesting features of FSS is gain enhancement when it combines with Fabry - Perot

Cavity (FPC) which can be very useful for reconfigurable antenna (RA). As it exhibits many advantages in gain and efficiency, a combination of FSS, FPC, and RA, which suffer from power loss in active components and DC bias line, is necessary for this type of antenna. Different types of implementations of FSS can be found in [10, 11]. In [10], a dual layer of FSS is used to support the dual-band slot antenna for gain improvement in both bands. While it showed 14.9 dBi and 14.0 dBi in 2.4 GHz and 5 GHz respectively, the height of the antenna, however, is greatly increased by the implementation of the dual layer. In [11], the authors presented only a single layer FSS and create a Fabry - Perot cavity with dual polarization (horizontal and vertical) patch antenna surrounding with metasurface. Despite the great gain performance of 17.6 dBi and 19 dBi at 8.45 and 9.8 GHz respectively, the design suffers from its large size ($3.7\lambda \times 3.7\lambda$ at 8.45 GHz). Recently, many researchers are focusing on reconfigurable metasurface, which will use numerous active components [12]. However, the structure's complexity may become its drawback.

In this paper, we propose a reconfigurable microstrip patch antenna operating in two different modes, i.e., circular polarization at 1.8 GHz and linear polarization at 2.45 GHz, and incorporating an FSS structure for gain enhancement. The proposed design aims to achieve similar gains at both bands so that a large number of devices working at both bands can cover the shadow area and provide pervasive communications [13, 14].

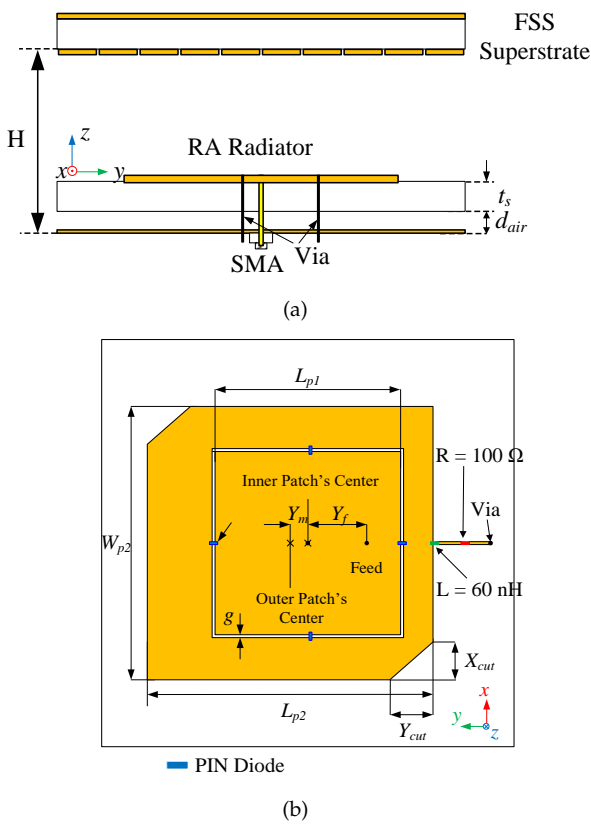


Figure 1. Design of RA-FSS antenna (a) Front view and (b) Top view of the RA radiator. ($L_{p1} = W_{p1} = 35$, $L_{p2} = W_{p2} = 52.5$, $Y_f = 8.5$, $Y_m = 4.5$, $X_{cut} = 6.5$, $Y_{cut} = 7$, $t_s = 1.6$, $d_{air} = 1.6$, $H = 70$). (Unit: mm)

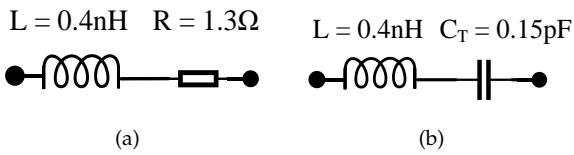


Figure 2. Equivalent circuit of PIN Diode (a) Mode ON (b) Mode OFF.

The structure of the paper is as follows. Section 2 describes the structure and analysis of the proposed antenna. Section 3 will show the comparison of simulation and measurement results. Lastly, section 4 is the conclusion of the antenna design.

2 ANTENNA DESIGN AND ANALYSIS

2.1 Dual Ring Reconfigurable Antenna

The main radiator is a polarization and frequency reconfigurable microstrip patch antenna designed on a 1.6 mm FR-4 substrate. In the RA design, 4 PIN Diodes connect the inner square patch and outer ring having its center slightly offset for impedance matching (Figure 1). PIN Diode has two operating modes: mode ON which connects the inner patch and outer ring, and mode OFF isolating them. Each mode is simulated separately by using PIN diode’s equivalent circuit of the corresponding mode (Figure 2). An air gap is inserted between FR-4 substrate and ground plane to improve the gain performance of the proposed antenna [15].

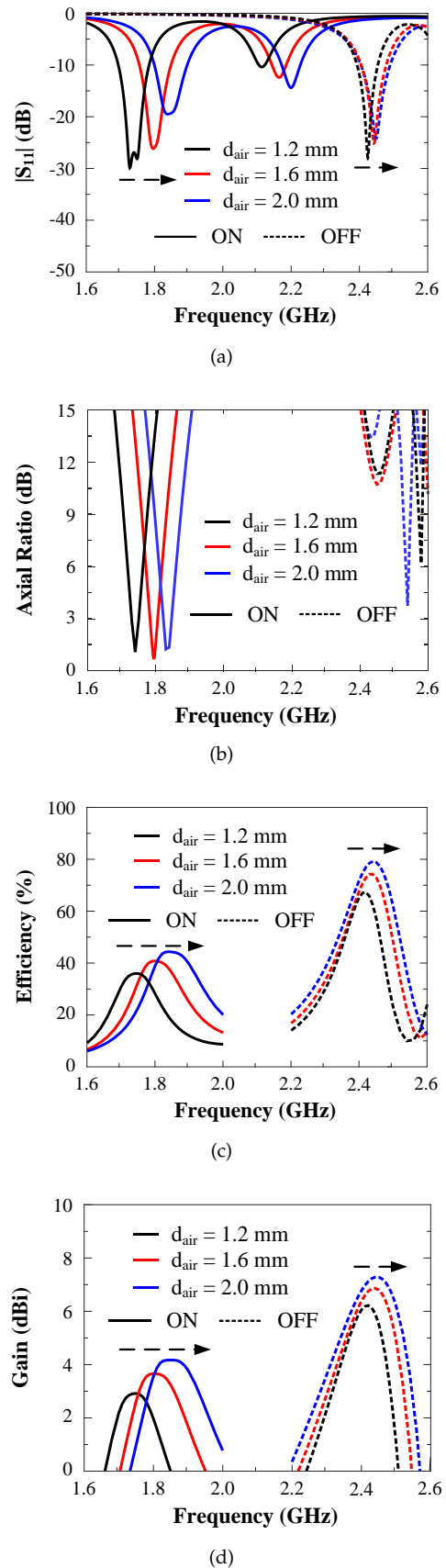


Figure 3. Parameter sweep of d_{air} (a) $|S_{11}|$, (b) Axial Ratio, (c) Efficiency, and (d) Broadside gain.

As illustrated in Figure 3, a parameter sweep of the said air gap d_{air} is performed. It is noted that this parameter affects greatly both bands due to the change

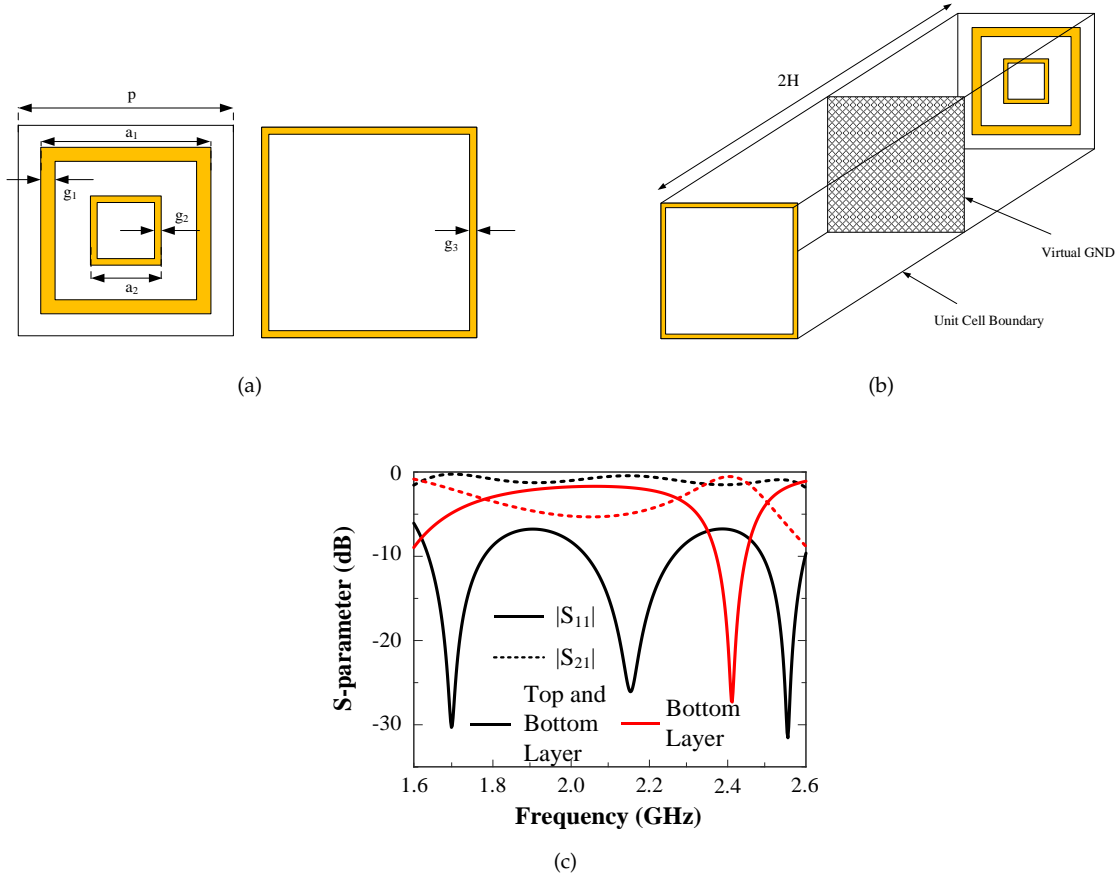


Figure 4. (a) FSS unit cell, (b) Simulation model, (c) S-parameters. ($p = 25$, $a_1 = 17.5$, $a_2 = 7.4$, $g_1 = 0.2$, $g_2 = 1$, $g_3 = 0.2$, $H = 70$). (Unit: mm)

of effective permittivity according to formula (1) [16]:

$$\epsilon_{eff} = \frac{\epsilon_{r1}t_s + \epsilon_{r2}d_{air}}{t_s + d_{air}}, \quad (1)$$

where ϵ_{r1} and ϵ_{r2} the relative permittivity of the FR-4 substrate and air respectively ($\epsilon_{r1} = 4.3$, $\epsilon_{r2} = 1$). Within only a step size of 0.4 mm from 1.2 mm to 2.0 mm, the operating frequency changes greatly in all performance (i.e., S_{11} , AR, Gain, and Efficiency). It should be noted that each band can be tuned separately based on formula (2) [17]

$$f = \frac{c}{2L\sqrt{\epsilon_{eff}}}, \quad (2)$$

where c is the light velocity in free space and the value of parameter L depends on the operating mode of PIN Diode. For instance, when PIN Diode is OFF, the coaxial cable only feeds the inner patch and thus, the value of parameter L is L_{p1} . The same can be concluded in the case of mode ON, which connects the inner patch and outer ring, meaning that the value of L_{p2} should be used in formula (2). It can be noted the frequency shift in both bands is not similar. When values of d_{air} are 1.2, 1.6 and 2.0, ϵ_{eff} are 2.9, 2.7 and 2.5 respectively. It should be noted that the effect of d_{air} is different for each band despite sharing the same value of effective dielectric constant. According to (2), the resonant frequency will depend on both ϵ_{eff} and L whose value is higher in ON state than OFF state. As a result, the change in resonant frequency in the lower band will be larger than

the higher one. According to the results in Figure 3, the parameter d_{air} is fixed at 1.6 mm to achieve the resonant frequency for GSM (1.8 GHz) and WiFi (2.45 GHz).

2.2 FSS Unit Cell

The other part of the proposed design is an FSS array. The superstrate also uses FR-4 as material and is placed over the ground plane at a distance of H to form a Fabry-Perot cavity. Because of the dual-band operation of the RA, the FSS array is designed to support both 1.8 GHz and 2.45 GHz for gain enhancement. In the proposed FSS design, the array is characterized by a unit cell that has a dual ring on the bottom side and a single ring on the top side (Figure 4(a)). The ring on the top layer acting as a resistive element [18] along with the dual ring on the bottom layer creates a wideband FSS to cover both bands. Each unit cell is duplicated over the same periodicity p in the x- and y-direction forming a 9×9 array.

The performance of the FSS unit cell is simulated using the model in Figure 4(b). Fabry - Perot Cavity mode is based on in-phase bouncing between the FSS array (superstrate) and the ground plane. In other words, the ground plane acts as a mirror that reflects the incoming wave. Therefore, to extract only the properties of the unit cell, the ground plane is removed and a mirrored model of the unit cell is added to imitate the bouncing behavior. According to Figure 4(c), using only the dual ring on the bottom layer can only support antenna

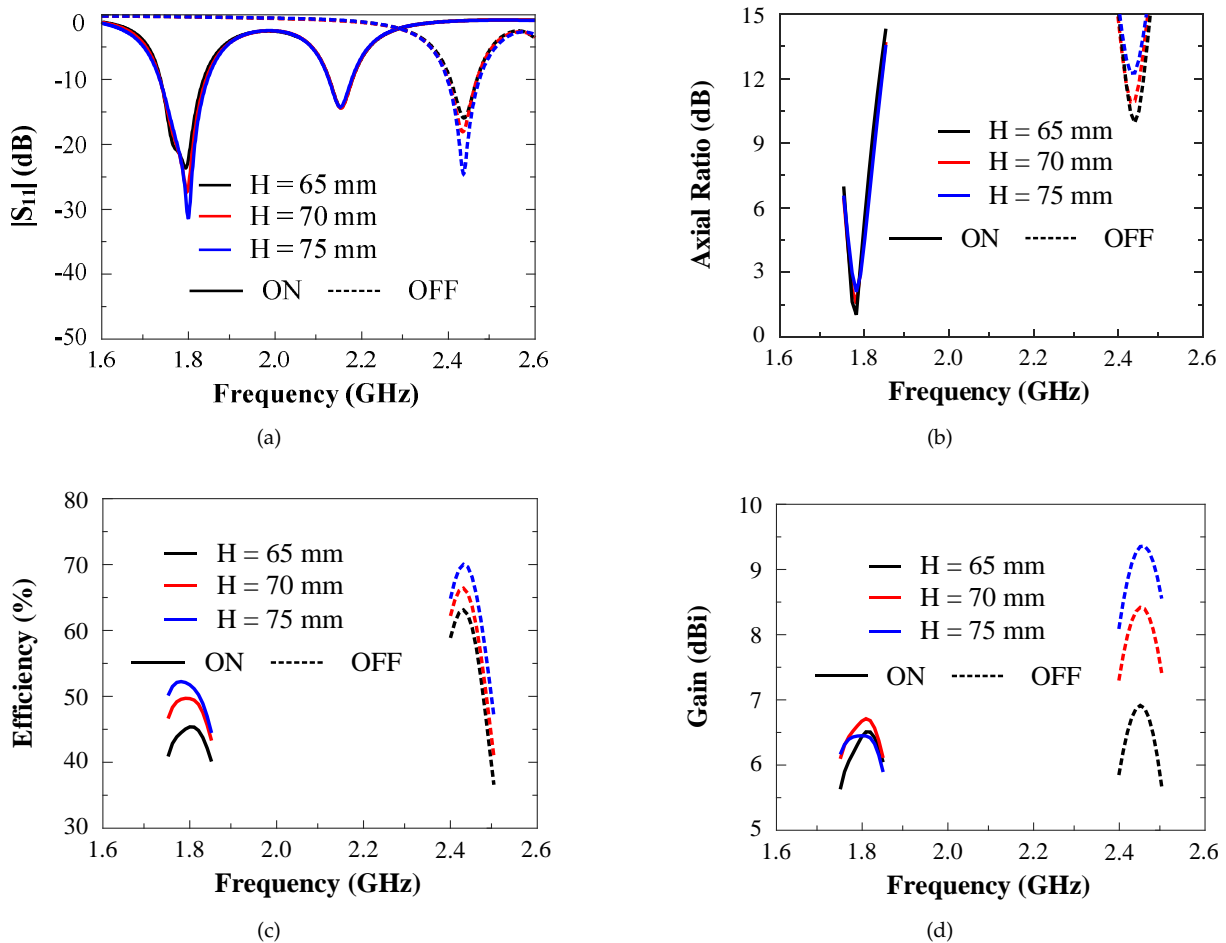


Figure 5. Parameter sweep of H ($n = 8$) (a) $|S_{11}|$, (b) Axial Ratio (AR), (c) Efficiency, (d) Gain.

performance at 2.45 GHz by having low reflection (i.e., S_{11}) and high transmission (i.e., S_{21}). With the addition of a resistive FSS ring on the top layer, the bandwidth of the FSS array is greatly enhanced and thus, suitable to improve gain at both 1.8 GHz and 2.45 GHz.

2.3 Reconfigurable Antenna and FSS Array

The RA-FSS with two important parameters, i.e., the cavity length H and the number of unit cells n , should be chosen carefully to obtain similar high gain characteristics in both bands. It is essential to note that since this is a dual-band antenna which is contradict to single operating frequency of the conventional Fabry - Perot cavity, the cavity length H will provide the best results in the medium value.

As shown in Figure 5, this parameter does not affect S_{11} and AR as greatly as gain performance. While S_{11} and AR present slight changes, gain performance is varied greatly between values. Though $H = 75$ mm gives a better gain in 2.45 GHz which is inversely in 1.8 GHz, cavity distance $H = 70$ mm is chosen as the optimal value for the best performance in both bands.

The other important design parameter is the number of unit cells n . Similar to the cavity length H , the number of unit cells n strongly affects gain performance, especially the lower band of 1.8 GHz. From simulation results in Figure 6(d), $n = 9$ is shown to be the saturated

value of the parameter since $n = 10$ does not show any improvement, and thus an FSS array of 9×9 unit cells is chosen in the final design.

From the above-observed results, it can be seen that the cavity length H and the number of unit cells n should be carefully chosen not only to improve the gain but also to achieve the similar high-gain characteristic at both frequency bands, i.e., 1.8 GHz and 2.45 GHz.

Figure 7 shows surface current distributions in both terms of direction and power at 2.45 GHz for linear polarization. Compared to 0° state, there is little power at 90° , 270° while the direction of current is opposite at 180° . This distribution presents a full cycle of a sinusoid wave and proves that the proposed antenna has linear polarization despite the non-ideal value of AR, which is about 10 dB. On the other hand, when PIN Diode is ON, the proposed antenna exhibits CP at 1.8 GHz, which is illustrated in Figure 8. Within a quarter of a full cycle, i.e., 90° , surface current rotates counter-clockwise, which is an indication of right-hand CP radiation.

Figure 9 shows the simulated co- and cross-polarization pattern of the proposed antenna. In both cases with and without FSS, simulation results illustrate a clear distinction between co- and cross-polarization. Specifically, a difference of about 12 dB is found on both states of PIN Diodes.

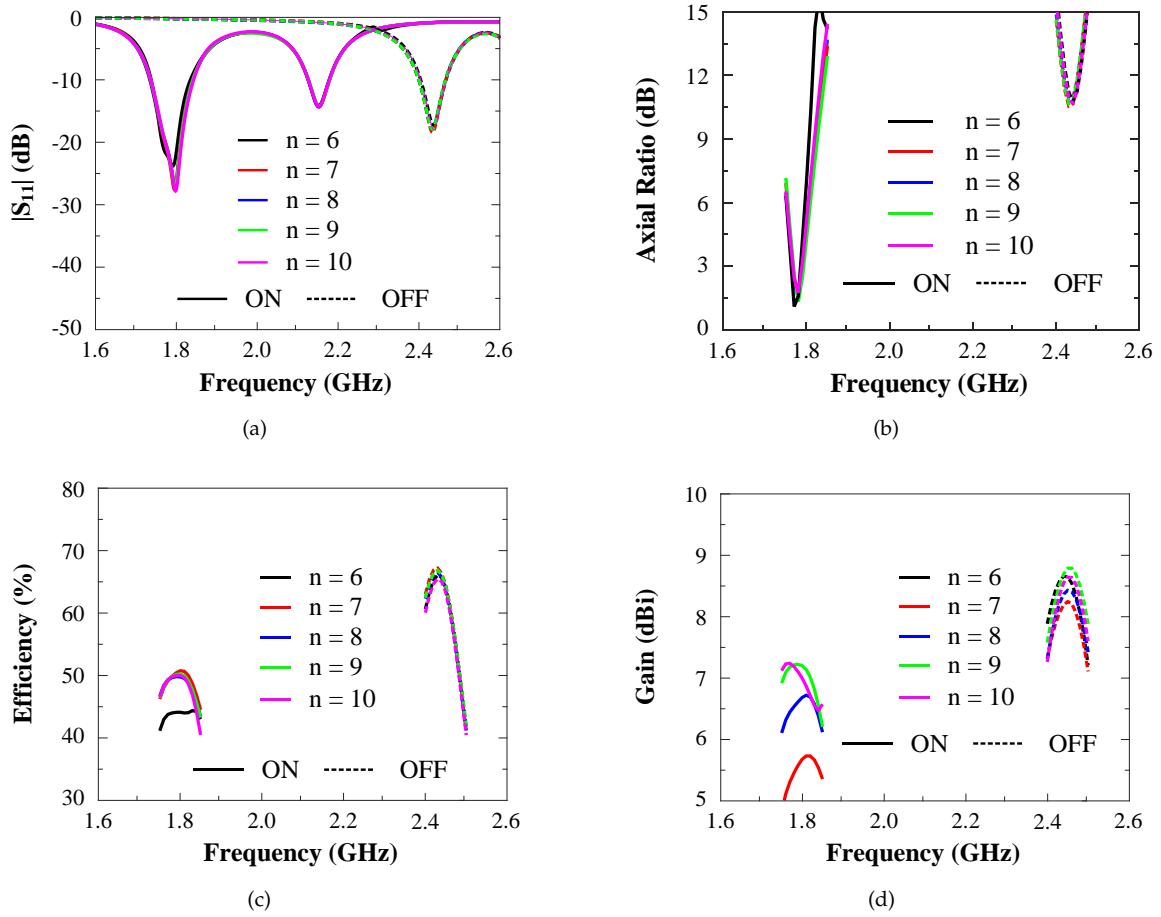


Figure 6. Parameter sweep of a number of unit cell n (a) $|S_{11}|$, (b) Axial Ratio (AR), (c) Efficiency, (d) Gain.

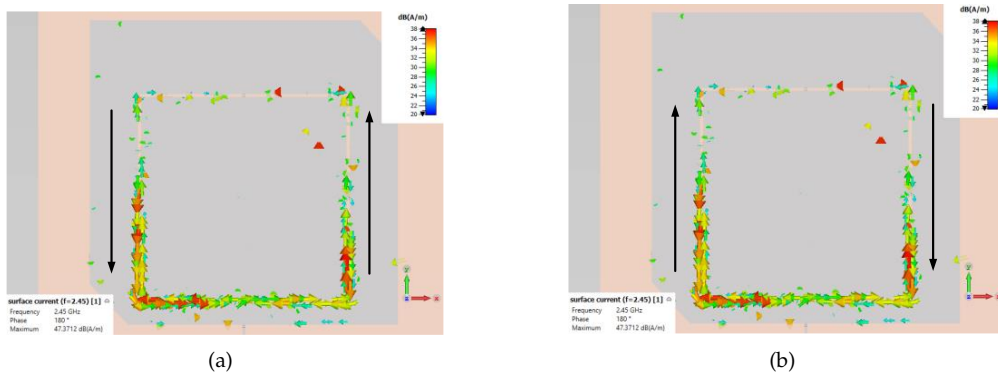


Figure 7. Surface current distribution of the proposed antenna when PIN Diode is OFF at 2.45 GHz at (a) 0° and (b) 180° to verify linear polarization.

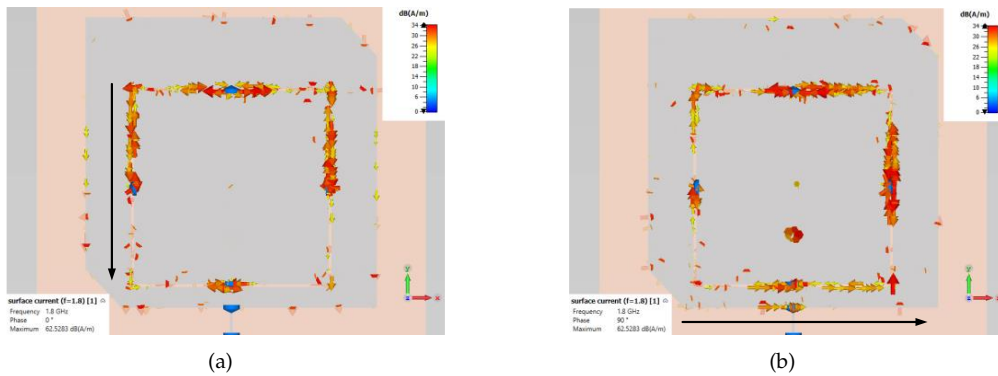


Figure 8. Surface current distribution of the proposed antenna when PIN Diode is ON at 1.8 GHz at (a) 0° and (b) 90° to verify circular polarization.

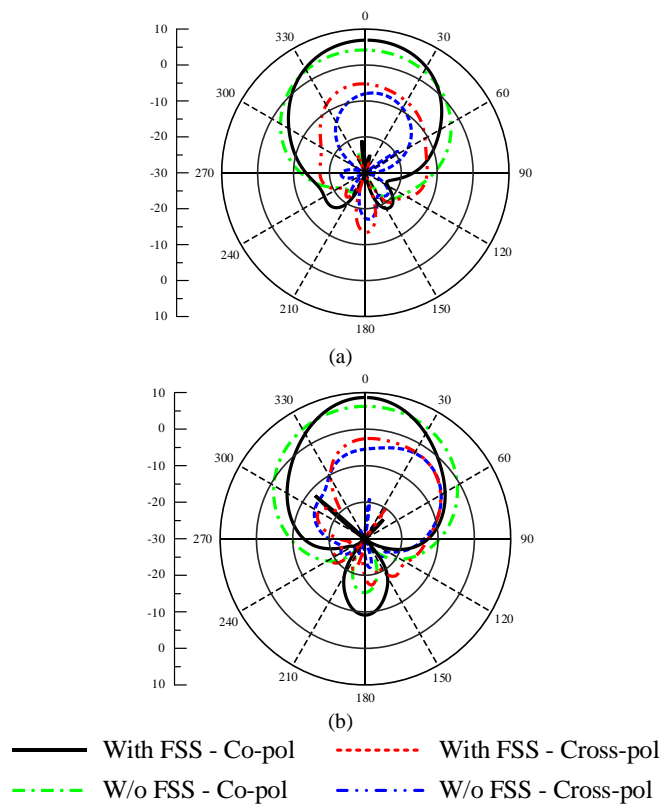


Figure 9. Simulated Co- and Cross-polarization patterns of antenna (a) Mode ON at 1.8 GHz (b) Mode OFF at 2.45 GHz.

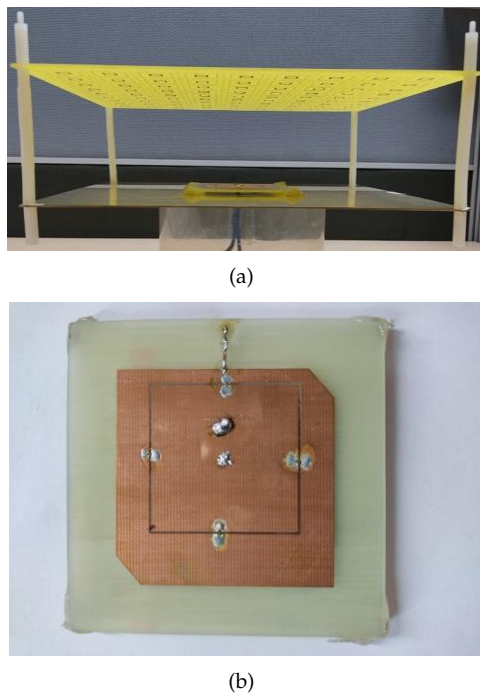


Figure 10. Fabricated antenna (a) Front view (b) Top view of the RA radiator.

3 SIMULATION AND MEASUREMENT RESULTS

The prototype of the RA-FSS antenna is fabricated using PIN Diode MADP-042305-130600 and RF inductor LQW04CA60NK00D as seen in Figure 10. Overall, it can be seen in Figure 11 that a good agreement was found between the simulation and measurement.

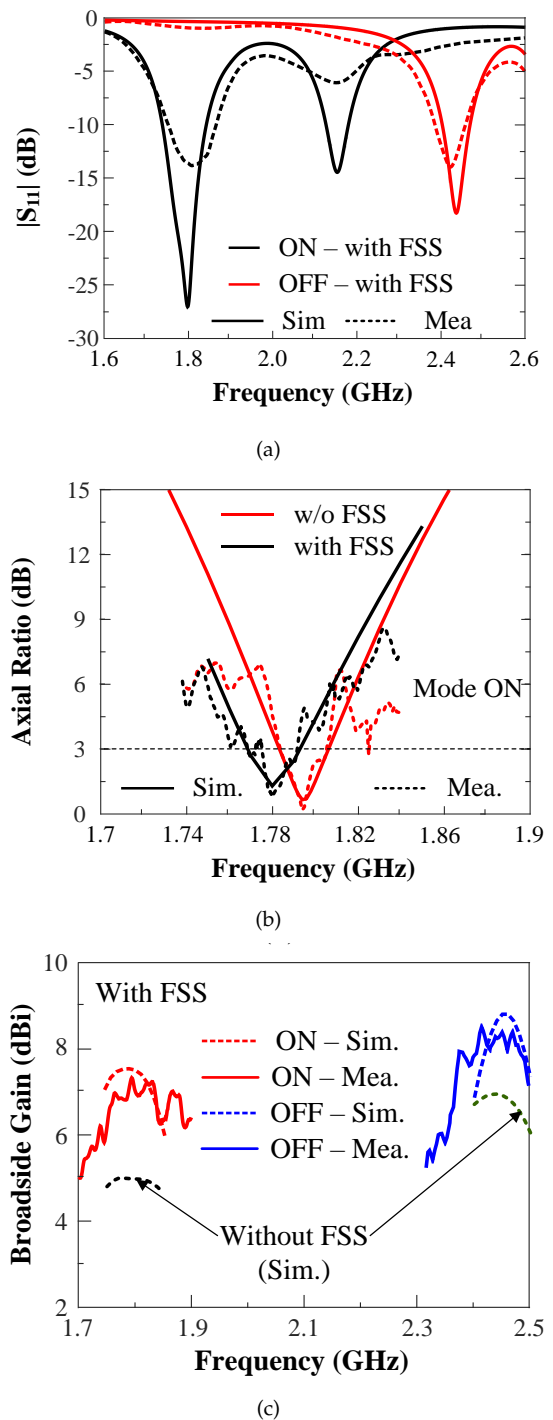


Figure 11. Comparison of simulation and measurement results (a) $|S_{11}|$, (b) AR when PIN Diodes are ON, (c) Broadside gain.

Measured resonant frequencies of mode ON (1.8 GHz) are slightly higher than the simulated one while those of mode OFF (2.45 GHz) is slightly lower, as seen in Figure 11 (a). Nevertheless, S_{11} of better than -10 dB is still maintained for both 1.8 GHz and 2.45 GHz bands. For the CP performance, however, the presence of FSS creates a slight frequency shift of about 0.01 GHz in simulated AR performance. Fortunately, as seen in Figure 11(b), the measured AR at 1.8 GHz still achieves about 3 dB to guarantee the CP characteristic. Finally, the comparison between the simulated and measured broadside gain is illustrated in Figure 11(c). Compared

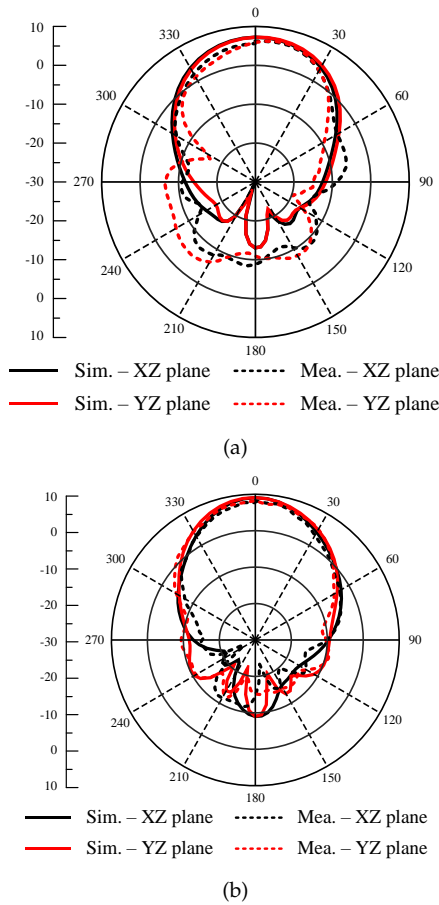


Figure 12. Simulated and measured radiation pattern of the proposed RA-FSS antenna at two modes (a) Mode ON at 1.8GHz, (b) Mode OFF at 2.45 GHz.

to a single microstrip antenna, the proposed design shows an improvement of about 2.2 dB at 1.8 GHz and about 1.8 dB at 2.4 GHz. The measured peak gain achieves a similar value goal of 7.2 dBi and 8.5 dBi. The measured peak gains, which achieve similar value goals of 7.2 dBi and 8.5 dBi are comparable to the simulated ones of 7.6 dBi and 8.8 dBi at 1.8 GHz and 2.45 GHz, respectively. It is noted that the simulated radiation efficiencies are about 50.6 % when diode ON (1.8 GHz) and about 66% when diode OFF (2.45 GHz).

Figure 12 compares the simulated and measured radiation patterns of the proposed RA-FSS antenna at two operating frequencies, which are obtained by MegiQ RMS-0704 measurement system. It can be seen that the measured and simulated radiation patterns are similar where the side-lobe-level (SLL) and front-to-back (FB) ratio of the simulation are slightly better than the measurement. The reduced radiation efficiency, and consequently the antenna gain, is attributed to the low-cost and high-loss FR-4 substrate and in addition to the switching losses seen by PIN diodes.

FPC design can also be evaluated by using aperture efficiency. According to [19], antenna aperture efficiency can be calculated based on G_{\max} as follow

$$G_{\max} = \left(\frac{4\pi}{\lambda_0^2}\right) A_{\text{eff}} E_f \quad (3)$$

with A_{eff} is effective area ($225 \times 225 \text{ mm}^2$) and E_f is

radiation efficiency. According to (3), G_{\max} at 1.8 GHz and 2.45 GHz are 11.45 and 28 dBi which account for 63% and 32% respectively. The low aperture efficiency in the higher band is due to the requirement of similar gain in both bands while using the same area as the lower band.

4 CONCLUSION

A frequency/polarization reconfigurable antenna incorporating FSS (RA-FSS) to achieve dual-band and similar high-gain characteristics at 1.8 GHz and 2.45 GHz is presented. Comparison between measurement and simulation results shows a good agreement in $|S_{11}|$, AR, and broadside gain performance. The proposed RA-FSS can exhibit the dual-band operation, linear/circular polarization reconfigurability, and similar high-gain characteristics while having an overall dimension of about $1.3\lambda \times 1.3\lambda \times 0.43\lambda$ (at 1.8 GHz). It can be concluded that the proposed RA-FSS antenna is not only suitable for GSM (1.8 GHz) and WiFi (2.45 GHz) applications but also suitable to be installed to reduce shadow area and provide reliable communications thanks to its similar high-gain characteristic.

ACKNOWLEDGMENT

This research is funded by Vietnam National Foundation for Science and Technology Development (NAFOS-TED) under Grant No. 102.04-2019.04.

REFERENCES

- [1] N. Ojaroudi Parchin, H. Jahanbakhsh Basherlou, Y. I. Al-Yasir, R. A. Abd-Alhameed, A. M. Abdulkhaleq, and J. M. Noras, "Recent developments of reconfigurable antennas for current and future wireless communication systems," *Electronics*, vol. 8, no. 2, p. 128, 2019.
- [2] N. Ojaroudi Parchin, H. Jahanbakhsh Basherlou, Y. I. Al-Yasir, A. M. Abdulkhaleq, and R. A. Abd-Alhameed, "Reconfigurable antennas: Switching techniques – A survey," *Electronics*, vol. 9, no. 2, p. 336, 2020.
- [3] P. T. Minh, N. T. Duc, P. X. Vu, N. T. Chuyen, and V. Van Yem, "Low profile frequency reconfigurable pifa antenna using defected ground structure," *REV Journal on Electronics and Communications*, vol. 7, no. 1-2, 2017.
- [4] L.-Y. Ji, P.-Y. Qin, Y. J. Guo, C. Ding, G. Fu, and S.-X. Gong, "A wideband polarization reconfigurable antenna with partially reflective surface," *IEEE Transactions on Antennas and Propagation*, vol. 64, no. 10, pp. 4534–4538, 2016.
- [5] T. Zhang, S.-Y. Yao, and Y. Wang, "Design of radiation-pattern-reconfigurable antenna with four beams," *IEEE Antennas and Wireless Propagation Letters*, vol. 14, pp. 183–186, 2014.
- [6] G. V. Trentini, "Partially reflecting sheet arrays," *IRE Transactions on Antennas and Propagation*, vol. 4, no. 4, pp. 666–671, 1956.
- [7] H. Zhu, X. Liu, S. Cheung, and T. Yuk, "Frequency-reconfigurable antenna using metasurface," *IEEE Transactions on Antennas and Propagation*, vol. 62, no. 1, pp. 80–85, 2013.
- [8] T. Ali and R. C. Biradar, "A compact hexagonal slot dual band frequency reconfigurable antenna for WLAN

- applications," *Microwave and Optical Technology Letters*, vol. 59, no. 4, pp. 958–964, 2017.
- [9] A. Iqbal, A. Smida, L. F. Abdulrazak, O. A. Saraereh, N. K. Mallat, I. Elfergani, and S. Kim, "Low-profile frequency reconfigurable antenna for heterogeneous wireless systems," *Electronics*, vol. 8, no. 9, p. 976, 2019.
- [10] M. L. Abdelghani, H. Attia, and T. A. Denidni, "Dual-and wideband Fabry-Pérot resonator antenna for WLAN applications," *IEEE Antennas and Wireless Propagation Letters*, vol. 16, pp. 473–476, 2016.
- [11] P. Xie, G. Wang, X. Kong, and J. Li, "Design of a novel metasurface for dual-band Fabry-Pérot cavity antenna," *International Journal of RF and Microwave Computer-Aided Engineering*, vol. 28, no. 2, p. e21181, 2018.
- [12] P. Xie and G.-M. Wang, "Design of a frequency reconfigurable Fabry-Pérot cavity antenna with single layer partially reflecting surface," *Progress In Electromagnetics Research Letters*, vol. 70, pp. 115–121, 2017.
- [13] S. X. Ta, J. J. Han, H. Choo, and I. Park, "Dual-band printed dipole antenna with wide beamwidth for WLAN access points," *Microwave and Optical Technology Letters*, vol. 54, no. 12, pp. 2806–2811, 2012.
- [14] A. Gijo, S. Shynu, P. Mohanan, C. Aanandan, and K. Vasudevan, "Compact dual-band antenna for wireless access point," *Electronics Letters*, vol. 42, no. 9, p. 1, 2006.
- [15] S. Park, C. Kim, Y. Jung, H. Lee, D. Cho, and M. Lee, "Gain enhancement of a microstrip patch antenna using a circularly periodic ebg structure and air layer," *AEU-International Journal of Electronics and Communications*, vol. 64, no. 7, pp. 607–613, 2010.
- [16] K. Ozenc, M. E. Aydemir, and A. Öncü, "Design of a 1.26 GHz high gain microstrip patch antenna using double layer with airgap for satellite reconnaissance," in *Proceedings of the 6th International Conference on Recent Advances in Space Technologies (RAST)*. IEEE, 2013, pp. 499–504.
- [17] C. Balanis, *Antenna theory: analysis and design (4-th ed.)*. John Wiley & Sons, Inc, 2016.
- [18] Z.-G. Liu, W.-B. Lu, and W. Yang, "Enhanced bandwidth of high directive emission fabry-perot resonator antenna with tapered near-zero effective index using metasurface," *Scientific Reports*, vol. 7, no. 1, pp. 1–10, 2017.
- [19] A. K. Singh, M. P. Abegaonkar, and S. K. Koul, "High-gain and high-aperture-efficiency cavity resonator antenna using metamaterial superstrate," *IEEE Antennas and Wireless Propagation Letters*, vol. 16, pp. 2388–2391, 2017.



Cong Danh Bui received his BE degree in Telecommunication Engineering from Ho Chi Minh University of Technology, Vietnam in 2018, and his M.Tech in Communication Engineering from Ton Duc Thang University, Vietnam in 2022. From 2018 - 2022, he was working as Research Assistant of Professor Truong Khang Nguyen at Institute for Computational Science, Ton Duc Thang University, researching on designing reconfigurable, array antennas, and antennas using metamaterial.

He is currently pursuing his Ph.D. on the topic of "Flexible compostable antennas from sustainable materials" at CONNECT, with funding from SFI CONNECT Research Centre - Phase 2 Platform Funding. His research interests focus on designing compact chipless RFID sensors, reconfigurable antennas, developing electromagnetic model and measurement of compostable materials.



Minh Thuan Doan received his BE degree in Telecommunication Engineering from Ho Chi Minh University of Technology, Vietnam in 2019. His major in university is Electronics and Telecommunications. He worked at Thales Research & Technology for 6 months as an intern in 2019. During internship time, he did research about metamaterial using structured dielectric material. His current research is mainly focused on analyzing reconfigurable antenna structures.



Thi Thanh Kieu Nguyen received the B.S. degree in Computational Physics from Dalat University, Dalat City, Vietnam in 2008, and the M.S. degree in Radio Physics and Electronics - Engineering Physics from the University of Science, Vietnam National University, Ho Chi Minh City in 2015. She is currently Lecturer at Faculty of Engineering, Binh Thuan College in Binh Thuan, Vietnam.



Truong Khang Nguyen (Member IEEE) received the B.S. degree in Computational Physics from the University of Science, Vietnam National University, Ho Chi Minh City in 2006, and the M.S. and Ph.D. degrees in Electrical and Computer Engineering from Ajou University in Suwon, Korea in 2013. From Oct. 2013 to Dec. 2014, he worked at Division of Energy Systems Research, Ajou University, Korea as a postdoctoral fellow. He is currently Assistant Director, and also Head of Division

of Computational Physics at Institute for Computational Science, Ton Duc Thang University in Ho Chi Minh City, Vietnam. His current research interests include microwave antennas for wireless communication, terahertz antennas for compact and efficient sources, nanostructures and nanoantennas for optical applications, and computational micro/nano structures.